nature biotechnology

LETTERS

Integrated barcode chips for rapid, multiplexed analysis of proteins in microliter quantities of blood

Rong Fan[1–3,5], Ophir Vermesh[1–3,5], Alok Srivastava[1,4], Brian K H Yen[1–3], Lidong Qin[1–3], Habib Ahmad[1–3], Gabriel A Kwong[1–3], Chao-Chao Liu[1–3], Juliane Gould[1–3], Leroy Hood[1,4] & James R Heath[1–3]

As the tissue that contains the largest representation of the human proteome[1], blood is the most important fluid for clinical diagnostics[2–4]. However, although changes of plasma protein profiles reflect physiological or pathological conditions associated with many human diseases, only a handful of plasma proteins are routinely used in clinical tests. Reasons for this include the intrinsic complexity of the plasma proteome[1], the heterogeneity of human diseases and the rapid degradation of proteins in sampled blood[5]. We report an integrated microfluidic system, the integrated blood barcode chip that can sensitively sample a large panel of protein biomarkers over broad concentration ranges and within 10 min of sample collection. It enables on-chip blood separation and rapid measurement of a panel of plasma proteins from quantities of whole blood as small as those obtained by a finger prick. Our device holds potential for inexpensive, noninvasive and informative clinical diagnoses, particularly in point-of-care settings.

Microfluidics has permitted the miniaturization of conventional techniques to enable high-throughput and low-cost measurements in basic research and clinical applications[6,7]. Systems for biomolecular assays[8,9] and bio-separations[10,11], including the separation of circulating tumor cells or plasma from whole blood[12–14], have been reported. We developed the integrated blood barcode chip (IBBC) to address the need for microchips that integrate on-chip plasma separations from microliter quantities of whole blood with rapid *in situ* measurements of multiple plasma proteins. The immunoassay region of the chip is a microscopic barcode, integrated into a microfluidics channel and customized for the detection of many proteins and/or for the quantification of a single or few proteins over a broad concentration range. We demonstrate versatility of this barcode immunoassay by detecting human chorionic gonadotropin (hCG) from human serum over a 10^5 concentration range and by stratifying 22 cancer patients via multiple measurements of a dozen blood protein biomarkers for each patient. We also use the IBBC to assay a blood protein biomarker panel from whole human blood, performing all key steps in the immunoassay within 10 min of blood collection by finger prick.

We first present an overview of the IBBC and then discuss control of assay sensitivity, extension of a single protein assay to an assay for a large panel of biomarkers and, finally, integration of plasma separation from whole blood, followed by the rapid measurement of a panel of protein biomarkers. **Figure 1** shows the design of an IBBC for blood separation and *in situ* protein measurement. We designed a polydimethylsiloxane (PDMS)-on-glass chip to perform 8–12 separate multiprotein assays sequentially or in parallel, starting from whole blood.

The Zweifach-Fung effect describes highly polarized blood cell flow at branch points of small blood vessels[14–16]. A component of the IBBC, redesigned from a previous report[14], exploits this hydrodynamic effect by flowing blood through a low-flow-resistance primary channel with high-resistance, centimeter-long channels that branch off it at right angles (**Fig. 1a**). As the resistance ratio is increased between the branches and the primary channel, a critical streamline moves closer to the primary channel wall adjoining the branch channels. Blood cells with a radius larger than the distance between this critical streamline and the primary channel wall are directed away from the high-resistance channels, and ~15% of the plasma is skimmed into the high-resistance channels. The remaining whole blood is directed toward a waste outlet. The glass base of the plasma-skimming channels is patterned with a dense barcode-like array of single-stranded DNA (ssDNA) oligomers before assembly of the microfluidics chip. A full barcode is repeated multiple times within a single plasma-skimming channel, and each barcode sequence constitutes a complete assay.

We used the DNA-encoded antibody library (DEAL) technique[17] (**Supplementary Fig. 1** online) to detect proteins within the plasma-skimming channels. DEAL technology involves using DNA-directed immobilization of antibodies to convert a prepatterned ssDNA barcode microarray into an antibody microarray, thereby providing a powerful means for spatial encoding[18,19]. The sequences of all ssDNA oligomer pairs used (labeled A/A′-M/M′), and their corresponding antibodies, are listed in **Supplementary Tables 1** and **2** online. To minimize cross-reactivity, these ssDNA molecules were designed *in silico* and then validated through a full orthogonality test (**Supplementary Fig. 2** online). In that experiment, each of the complementary DNA molecules with Cy3 fluorescent label was added to a

[1]NanoSystems Biology Cancer Center, [2]Kavli Nanoscience Institute, [3]Division of Chemistry and Chemical Engineering, California Institute of Technology, MC 127-72, 1200 E. California Blvd., Pasadena, California 91125, USA. [4]Instititue for Systems Biology, 1441 North 34th St., Seattle, Washington 98103-8904, USA. [5]These authors contributed equally to this work. Correspondence should be addressed to J.R.H. (heath@caltech.edu).

Received 21 July; accepted 21 October; published online 16 November 2008; doi:10.1038/nbt.1507

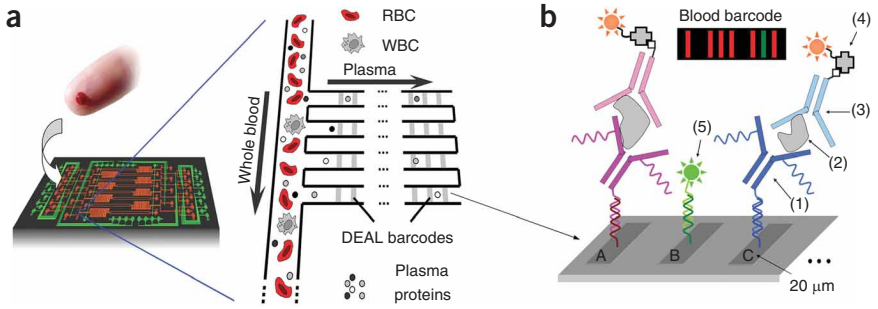

Figure 1 Design of an integrated blood barcode chip (IBBC). (**a**) Scheme depicting plasma separation from a finger prick of blood by harnessing the Zweifach-Fung effect. Multiple DNA-encoded antibody barcode arrays are patterned within the plasma-skimming channels for *in situ* protein measurements. (**b**) DEAL barcode arrays patterned in plasma channels for *in situ* protein measurement. A, B, C indicate different DNA codes. (1)–(5) denote DNA-antibody conjugate, plasma protein, biotin-labeled detection antibody, streptavidin-Cy5 fluorescence probe and complementary DNA-Cy3 reference probe, respectively. The inset represents a barcode of protein biomarkers, which is read out using fluorescence detection. The green bar represents an alignment marker.

microwell containing a full primary ssDNA barcode array. The results showed only negligible cross-hybridization signals. In the DEAL assay, each capture antibody is tagged with approximately three copies of an ssDNA oligomer that is complementary to ssDNA oligomers that have been surface-patterned into a microscopic barcode within the immunoassay region of the chip. Flow-through of the DNA-antibody conjugates transforms the DNA microarray into an antibody microarray for the subsequent surface-bound immunoassay. Because DNA patterns are robust to dehydration and can survive elevated temperatures (80–100 °C), the DEAL approach circumvents the denaturation of antibodies often associated with typical microfluidics fabrication.

As only a few microliters of blood is normally sampled from a finger prick, on-chip plasma separation yields only a few hundred nanoliters of plasma. The ssDNA barcodes were patterned at a high density using microchannel-guided flow patterning (**Supplementary Fig. 3** online) to measure a large panel of protein biomarkers from this small volume. We used a PDMS mold that was thermally bonded onto a polyamine-coated glass slide to pattern the entire ssDNA barcode. Polyaminated surfaces permit substantially higher DNA loading than do more traditional aminated surfaces[20] and provide for an accompanying increase in assay sensitivity (**Supplementary Figs. 4** and **5** online). Different solutions, each containing a specific ssDNA oligomer, were flowed through different channels and evaporated through the gas-permeable PDMS stamp, resulting in individual stripes of DNA molecules. One complete set of stripes represents one barcode. All measurements used 20-μm-wide bars spaced at a 40 μm pitch. This array density represents an approximately tenfold increase over a standard spotted array (typical dimensions are 150 μm diameter spots at a 400 μm pitch), thus expanding the numbers of proteins that can be measured within a small volume. No alignment between the barcode array and the plasma channels (IBBC chip design presented in **Supplementary Fig. 6** online) was required. All protein assays used one color fluorophore and were spatially identified using a reference marker that fluoresced at a different color.

We first illustrate aspects of the barcode assays via the measurement of a single biomarker, human chorionic gonadotropin (hCG), in undiluted human serum over a broad concentration range. hCG is widely used for pregnancy testing and is a biomarker for gestational trophoblastic tumors and germ cell cancers of the ovaries and testes. For this assay, the barcode was customized by varying the DNA loading during the flow patterning step. The DNA barcode contained 13 regions (**Fig. 2a**). There were two bars of oligomer B (designed to detect the protein tumor necrosis factor (TNF)-α as a negative control), one reference bar (oligomer M), one blank and nine bars of oligomer A (designed for hCG detection and flow patterned at ssDNA concentrations that were varied from 200 μM to 2 μM). To perform the assay, we flowed a mixture of A′-anti-hCG and B′-TNF-α through assay channels. Next, a series of standard hCG serum samples and two hCG samples of unknown concentration were flowed through separate assay channels. Biotinylated detection antibodies for hCG and TNF-α were then applied, followed by a final developing step using

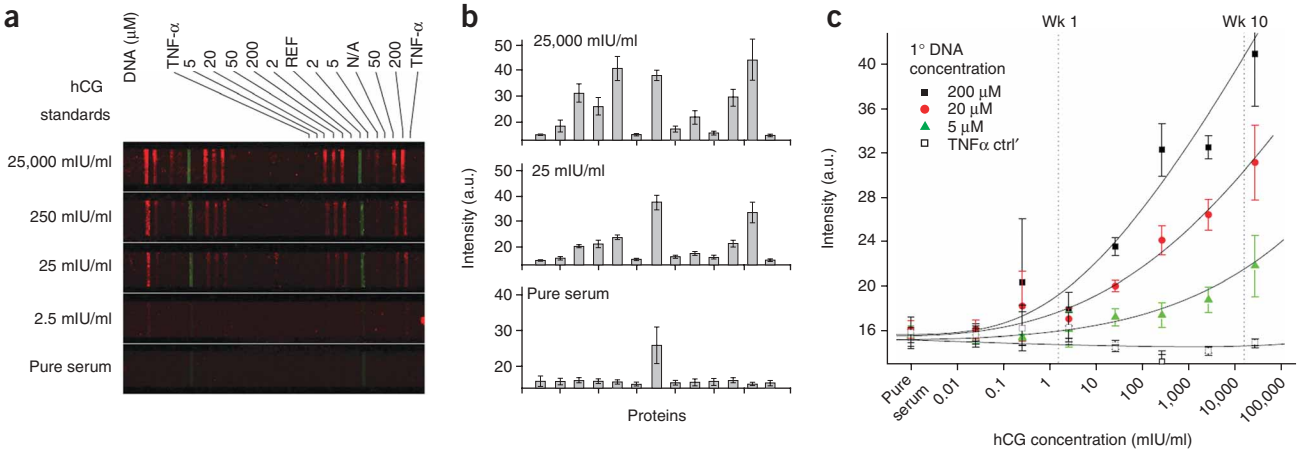

Figure 2 Measurement of human chorionic gonadotropin (hCG) in sera. (**a**) Fluorescence images of DEAL barcodes showing the measurement of a series of standard serum samples spiked with hCG. The bars used to measure hCG were patterned with DNA strand A at different concentrations. TNF-α encoded by strand B was employed as a negative control. The green bars (strand M) serve as references. (**b**) Quantification of the full barcodes for three selected samples. (**c**) Mean values of fluorescence signals corresponding to three sets of bars with different DNA loadings. Broken lines indicate the typical physiological levels of hCG in sera after 1 or 10 weeks of pregnancy. Error bars, 1 s.d.

fluorescent Cy5-labeled streptavidin (red) for all protein channels and Cy3-labeled M′ oligomers (green) for the reference channel (**Fig. 2a**). Quantifying the fluorescence intensity (**Fig. 2b,c**) revealed a sensitivity (~1 mIU/ml) comparable to the enzyme-linked immunosorbent assays (ELISAs) over a broad detected concentration range (~10^5). Using the microfluidics-entrained DEAL barcode in a blind test, we measured the hCG levels in the two unknown serum samples. Our measured levels, estimated at 6 and 400 mIU/ml for unknowns 1 and 2, are in good agreement with the values of 12 and 357 mIU/ml, respectively, obtained from an independent lab test (**Supplementary Fig. 7** online). Even without quantification, the analyte concentrations can be estimated by eye through pattern recognition of the full barcode. The bar with the highest DNA-loading rendered the highest sensitivity, whereas the bar with lowest DNA-loading was used to discriminate samples with high analyte concentrations. For example, the 25,000 mIU/ml and 250 mIU/ml hCG samples can be visually distinguished using stripes patterned with lower DNA concentrations, whereas the stripes loaded from 200 μm DNA solutions do not readily distinguish these samples. For circumstances in which accurate photon counting is not available, visual barcode inspection permits a rough estimation of the target quantity—a potential point-of-care application. When levels of hCG are tracked during pregnancy, concentrations in the blood increase from ~5 mIU/ml in the first week of pregnancy to ~2×10^5 mIU/ml 10 weeks after conception. The IBBC can cover such a broad physiological hCG range with reasonable accuracy.

To evaluate multiplexed measurements of a panel of 12 protein markers using the microfluidic DEAL barcode regions of the IBBCs, we quantified the cross-reactivity between the stripes within the DNA-encoded immunoassays. This test involved twelve human serum proteins, including ten cytokines (interferon (IFN)-γ, TNF-α, interleukin (IL)-2, IL-1α, IL-1β, transforming growth factor (TGF)-β1, IL-6, IL-10, IL-12, granulocyte-macrophage colony-stimulating factor (GM-CSF)), a chemokine macrophage chemoattractant protein (MCP)-1 and the cancer biomarker prostate-specific antigen (PSA). The results showed negligible cross-talk, with typical photon counts <2% compared to the correctly paired antigen-antibody complexes (**Supplementary Fig. 8** online). We also assayed serial dilutions (from 5 nM to 1 pM) for these proteins on the DEAL barcode chip to establish a set of calibration curves for future estimates of protein concentration in sera (**Supplementary Fig. 9** online). We fixed all the parameters associated with laser scanning and fluorescence quantification (e.g., power, gain, brightness and contrast) and performed quantitative analysis. Depending on the antibodies used, the estimated sensitivity varies from <1 pM for IL-1β and IL-12 to ~30 pM for TGF-β and is comparable to the detection limits of ELISAs based on the same antibody pairs. For example, according to the specifications of commercial kits (eBioscience), the detection limit for cytokines like TNF-α and IL-1β is ~8 pg/ml (~0.5 pM), which compares favorably with our observations. However, the statistical variation of the measured signals is relatively large compared to a commercial ELISA assay—a variation that likely arises from our manual chip manufacturing.

We assessed the utility of the DEAL barcodes for clinical blood samples by measuring the same 12 proteins from small amounts of stored serum collected from 22 cancer patients. These serum samples were thawed,

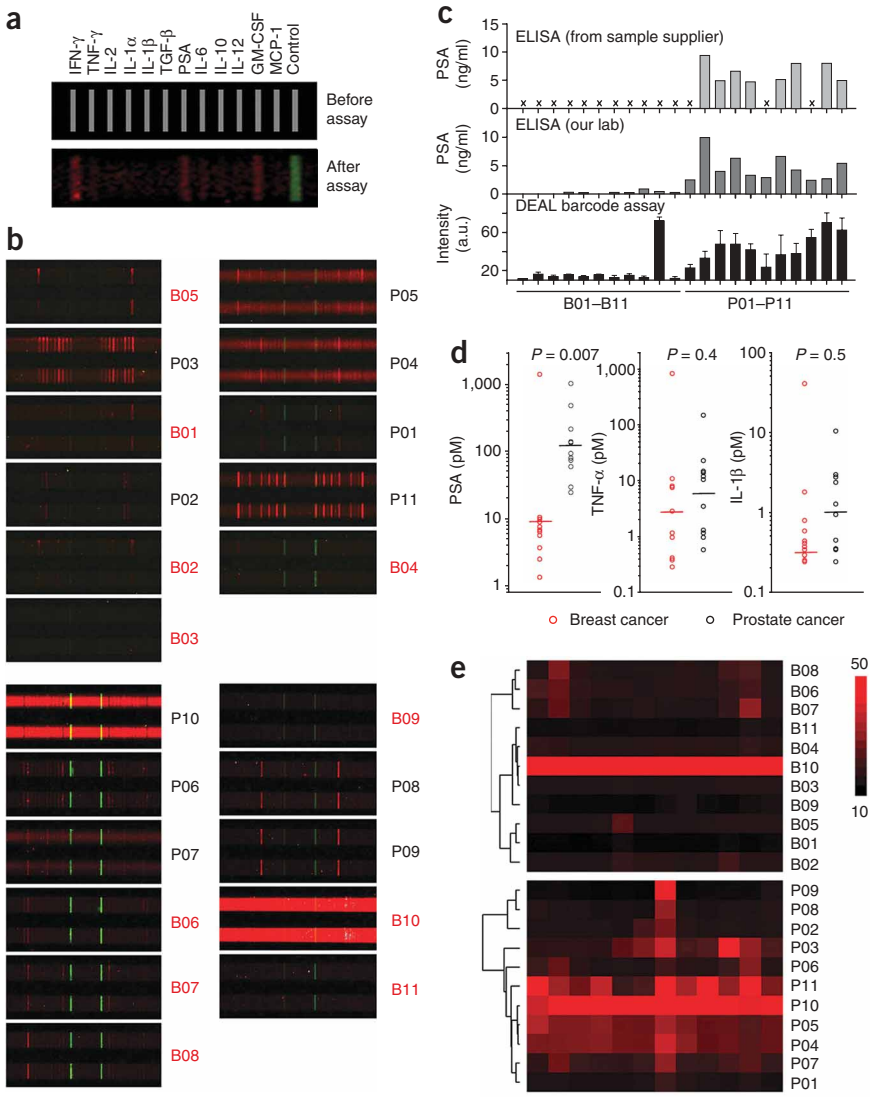

Figure 3 Multiplexed protein measurements of clinical patient sera. (**a**) Layout of the barcode array used in this study. Green denotes the reference (strand M). (**b**) Representative fluorescence images of barcodes used to measure the cancer marker PSA and 11 cytokines from 22 cancer patient serum samples. B01–B11, samples from breast cancer patients; P01–P11, samples from prostate cancer patients. The left and right columns represent measurements on different chips. (**c**) Validation of PSA DEAL barcode measurement using ELISA. x denotes PSA measurements were not provided by the serum supplier. Error bars, 1 s.d. (**d**) Distribution of estimated concentrations of PSA, TNF-α and IL-1β in all serum samples. The horizontal bars mark the mean values. (**e**) Complete nonsupervised clustering of breast and prostate cancer patients on the basis of protein patterns.

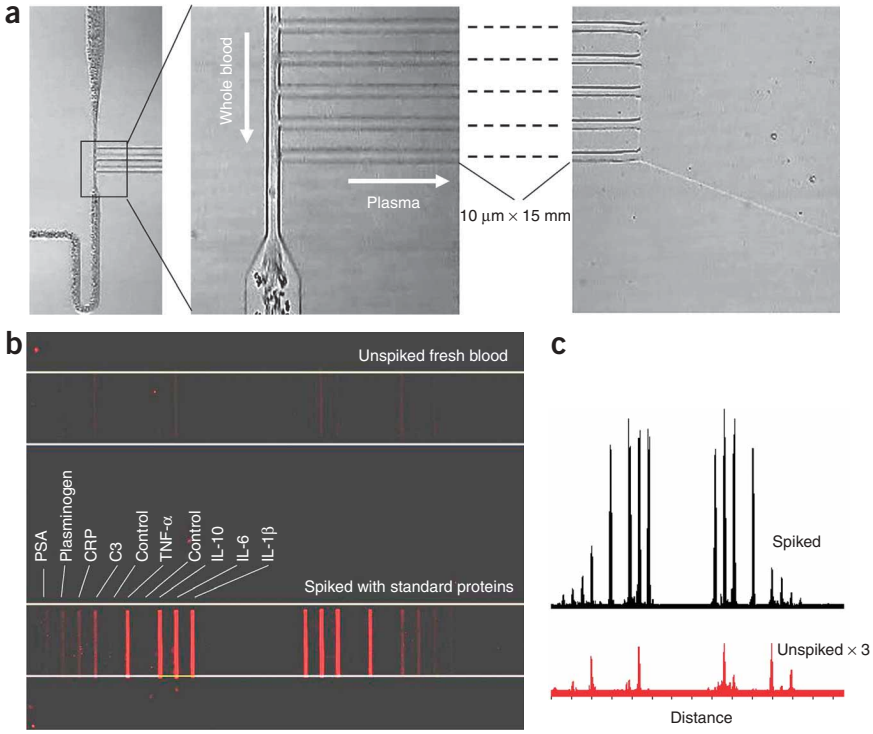

Figure 4 IBBC for the rapid measurement of a panel of serum biomarkers from a finger prick of whole blood. (**a**) Optical micrographs showing the effective separation of plasma from fresh whole blood. A few red blood cells occasionally seen downstream of the plasma channels did not affect the protein assay. (**b**) Fluorescence image of blood barcodes in two adjacent microchannels of an IBBC, on which both the unspiked and spiked fresh whole blood collected from a healthy volunteer were separately assayed. Eight plasma proteins are indicated. All bars, 20 μm wide. (**c**) Fluorescence line profiles of the barcodes for both unspiked and spiked whole blood samples. The distance corresponds to the full length shown in **b**.

and then assayed using two chips, each containing 12 separate assay units operated in parallel. In every unit, 20 full DEAL barcodes in each assay channel were used for statistical sampling. The proteins in this panel (**Fig. 3a**), the prostate cancer marker PSA and eleven proteins secreted by various white blood cells, have been associated with tumor microenvironment formation, tumor progression and tumor metastasis[21–23]. Thus, this panel provides information relevant to multiple aspects of cancer.

Figure 3b shows fluorescence images, each depicting four sets of randomly picked barcodes obtained from the 22 patient samples. The medical records for all patients are summarized in **Supplementary Table 3** online. B01–B11 denote 11 samples from breast cancer patients, whereas P01–P11 are from prostate cancer patients. Many proteins were successfully detected with high signal-to-noise ratios, and the barcode signatures are distinctive from patient to patient, excepting the assays on P05, P04, P10 and B10. These assays are from individuals who are heavy smokers (~11–20 cigarettes daily). Only one serum sample (P06) from a heavy smoker did not exhibit a high background. This high background may result from elevated blood content of the fluorescent protein carboxyhemoglobin, which has been shown relevant to the pathogenesis of lung diseases of smokers[24]. Although we have also measured high background in a number of stored serum samples, we have never measured a high background in assays from very freshly collected blood, as described below. The results imply that, at least for stored samples, some prepurification of the plasma or serum will be required to assay serum protein levels.

Barcode intensities were then quantified and the statistic mean value for each protein was computed (**Supplementary Figs. 10**, **11** and **12** online). The cancer marker PSA clearly distinguished between the breast cancer and the prostate cancer patients. The only exception was a false-positive result from B10 that had high nonspecific background. We independently validated our PSA measurements using the standard ELISA for PSA in all patient sera. For eight of the prostate cancer patients, we compared these results with clinical ELISA measurements provided by the serum supplier. The results (**Fig. 3c**) validated the applicability of the DEAL barcodes for assaying complex clinical samples. However, the statistical accuracy of the PSA barcode assay was not high, revealing only a modest linear correlation between the ELISA and DEAL (**Supplementary Fig. 13** online). Again, this is likely due to our manual chip manufacturing process. We are currently automating our barcode fabrication, assay execution and image quantification in an effort to bring statistical uncertainties to within 10–20%, which would be close to the state of the art.

The cancer patient barcode data could be analyzed for absolute protein levels by comparing those data against the barcode quantification plots (**Supplementary Fig. 9**). Results for PSA, TNF-α and IL-1β are shown in **Figure 3d**. PSA concentrations range from 22 pM to 1 nM (or 0.7 to 33 ng/ml) with a log-scale mean of 117 pM (3.8 ng/ml) for prostate cancer patients. The estimated PSA concentrations for breast cancer patient sera has a mean of 9.1 pM. PSA readily differentiates between these two patient groups with good statistical accuracy ($P = 0.0007$). Nevertheless, the absolute PSA levels measured by either the standard ELISA or by the barcode assay are below those determined by the clinical ELISA—a likely result of sample degradation during storage (**Fig. 3c**). As would be expected, neither TNF-α nor IL-1β allows prostate and breast cancer patients to be distinguished ($P = 0.4$ and 0.5, respectively at significance level 0.2). Our estimates of absolute protein levels indicate that the protein concentration ranges assessed by the DEAL barcode assay are clinically relevant for patient diagnostics. For example, the serum level of cytokines such as interleukins and tumor necrosis factors can reach ~10–100 pg/ml in cancer patients[25], ~500 pg/ml in rheumatoid arthritis patients and >1 ng/ml[26] in septic shock[27]. These levels can all be captured using the barcode assay format.

We performed a complete nonsupervised clustering (that is, using only the levels of assayed proteins without assigning any weight factors) of patients and generated the heat map (**Fig. 3e**) to assess the potential of this technology for patient stratification. This analysis is only presented as a proof of principle. Nevertheless, the results are encouraging. For example, the measured profiles of breast cancer patients can be classified into three subsets—noninflammatory, IL-1β positive and TNF-α/GMCSF positive ($P_{TNF\alpha} = 0.005$, $P_{GMCSF} = 0.04$ for the latter two subsets). The prostate cancer patient data were

classified into two major subsets based upon the inflammatory protein levels ($P_{TNF\alpha} = 0.016$, $P_{GMCSF} = 0.012$). The multiplexed measurement of cytokines[28] is relevant to cancer diagnostics and prognostics[29,30]. Our results demonstrate that IBBCs can be applied to the multiparameter analysis of human health-relevant proteins in serum.

The ultimate goal behind developing the IBBC was to measure the levels of a large number of proteins in human blood within a few minutes of sampling that blood, to avoid the protein degradation that can occur when plasma is stored. In a typical 96-well plate immunoassay, the biological sample of interest is added, and the protein diffuses to the surface-bound antibody. Under adequate flow conditions, diffusion is no longer important, and the only parameter that limits the speed of the assay is the protein/antibody binding kinetics (the Langmuir isotherm)[31], thus allowing the immunoassay to be completed in just a few minutes[32]. Flow through our plasma-skimming channels proceeds at velocities $> \sim 0.1$ mm sec^{-1} and can operate continuously and with near 100% efficiency unless the blood flow is clogged.

For whole blood analysis, the microfluidic channels of IBBCs were precoated with bovine serum albumin blocking buffer. The DNA barcodes were transformed into antibody barcodes as described above, and blood samples were flowed into the device within 1 min of finger-prick collection. The time from that finger prick to completion of blood flow through the device was ~9 min. We sampled both as-collected whole blood and protein-spiked blood from healthy volunteers. **Figure 4a** shows the effective separation of plasma in an IBBC (also see **Supplementary Video** online). The few red blood cells that did enter the plasma channels (**Fig. 4a**, right panel) did not affect the subsequent protein assay.

The plasma proteins detected in this whole-blood analysis experiment included a cancer marker (PSA), four cytokines and three other functional proteins (complement C3, C-reactive protein (CRP) and plasminogen) involved in the complement system, inflammatory response, fibrin degradation and liver toxicity (**Supplementary Tables 1** and **2**). After exposure of the barcode assay region to the separated, flowing plasma for 8 min, the detection antibody solution and the fluorescence probes were added to complete the assay. All proteins in the spiked blood were detected (**Fig. 4b,c**). Cytokines gave the strongest fluorescence signals because of higher affinities of their cognate antibodies. The measurement of the unspiked fresh blood established a baseline for a healthy volunteer, in which IL-6, IL-10, C3 and plasminogen were detected. Using IBBCs for the separation and analysis of very freshly collected blood consistently resulted in very clean DEAL barcodes, with little or no evidence of biofouling. We are planning a study to assess the importance of rapid measurements for obtaining accurate protein levels.

Our IBBC enables the rapid measurement of a panel of plasma proteins from a finger prick of whole blood. Integration of microfluidics and DNA-encoded antibody arrays enables reliable processing of blood and *in situ* measurement of plasma proteins within a time scale that is short enough to avoid most protein degradation processes that can occur in sampled blood. Use of the IBBC represents a minimally invasive, low-cost and robust procedure, and potentially represents a realistic clinical diagnostic platform.

METHODS

Micropatterning of barcode array. A PDMS mold containing 13–20 parallel microfluidic channels, with each channel conveying a different DNA oligomer as DEAL code, was fabricated by soft lithography. The PDMS mold was bonded to a polylysine-coated glass slide via thermal treatment at 80 °C for 2 h. The polyamine surfaces permit significantly higher DNA loading than do more traditional aminated surfaces. DNA 'bars' of 2 μm in width have been successfully patterned using this technique. In the present study, a 20-μm channel width was chosen because the fluorescence microarray scanner we used has a resolution of 5 μm. Nevertheless, the current design already resulted in a DNA barcode array an order of magnitude denser than conventional microarrays fabricated by pin-spotting. The coding DNA solutions (A-M for the cancer serum test and AA-HH for the finger-prick blood test) prepared in 1× PBS were flowed into individual channels, and then allowed to evaporate completely. Finally, the PDMS was peeled off and the substrate with DNA barcode arrays was baked at 80 °C for 2–4 h. The DNA solution concentration was ~100 μM in all experiments except in the hCG test, leading to a high loading of $\sim 6 \times 10^{13}$ molecules/cm^2 (assuming 50% was collected onto substrate).

Fabrication of IBBCs. The fabrication of PDMS devices for the IBBCs was accomplished through a two-layer soft lithography approach. The control layer was molded from a SU8 2010 negative photoresist (~20 μm in thickness) silicon master using a mixture of GE RTV 615 PDMS prepolymer part A and part B (5:1). The flow layer was fabricated by spin-casting the pre-polymer of GE RTV 615 PDMS part A and part B (20:1) onto a SPR 220 positive photoresist master at ~2,000 r.p.m. for 1 min. The SPR 220 mold was ~17 μm in height after rounding by thermal treatment. The control layer PDMS chip was then carefully aligned and placed onto the flow layer, which was still situated on its silicon master, and an additional 60 min thermal treatment at 80 °C was performed to enable bonding. Afterward, this two-layer PDMS chip was cut off the flow layer master and access holes were drilled. Finally, the two-layer PDMS chip was thermally bonded onto the barcode-patterned glass slide, yielding a completed integrated blood barcode chip (IBBC). In this chip, the DEAL barcode stripes are oriented perpendicular to the microfluidic assay channels. Typically, 8–12 identical units were integrated in a single chip with the dimensions of 2.5 cm × 7 cm.

Clinical specimens of cancer patient sera. The stored serum samples from 11 breast cancer patients (all female) and 11 prostate cancer patients (all male) were acquired from Asterand. Nineteen out of 22 patients were European-American and the remaining three were Asian, Hispanic and African-American. The medical history is summarized in **Supplementary Table 3**.

Collecting a finger prick of blood. The human whole blood was collected according to the protocol approved by the institutional review board of the California Institute of Technology. Finger pricks were performed using BD microtainer contact-activated lancets. Blood was collected with SAFE-T-FILL capillary blood collection tubes (RAM Scientific), which we prefilled with 80 μl of 25 mM EDTA solution. A 10 μl volume of fresh human blood from a healthy volunteer was collected in an EDTA-coated capillary, dispensed into the tube, and rapidly mixed by inverting a few times. The spiked blood sample was prepared in a similar way except that 40 μl of 25 mM EDTA solution and 40 μl of recombinant solution were mixed and pre-added in the collection tube. Then 2 μl of 0.5 M EDTA was added to bring the total EDTA concentration up to 25 mM.

Execution of blood separation and plasma protein measurement using IBBCs. The IBBCs were first blocked with the buffer solution for 30–60 min. The buffer solution prepared was 1% wt/vol bovine serum albumin fraction V (Sigma) in 150 mM 1× PBS without calcium/magnesium salts (Irvine Scientific). The fluid loading was conducted using a Tygon plastic tubing that is interfaced to the IBBC inlet with a 23 gauge metal pin. The Fluidigm solenoid unit was exploited to control the pressure on/off for both control valves and flow channels. A pressure of 8–10 p.s.i. was applied to actuate the valves, whereas the loading of fluid into assay channels was carried out with a lower pressure (0.5–3 p.s.i.) depending on the channel flow resistance and the desired flow rate. Then DNA-antibody conjugates (~50–100 nM) were flowed through the plasma assay channels for ~30–45 min. This step transformed the DNA arrays into capture-antibody arrays. Unbound conjugates were washed off by flowing buffer solution through the channels. At this step, the IBBC was ready for the blood test. Two blood samples prepared as mentioned above were flowed into the IBBCs within 1 min of collection. The IBBC quickly separated plasma from whole blood, and the plasma proteins of interest were

captured in the assay zone where DEAL barcode arrays were placed. This whole process from finger-prick to plasma protein capture took <10 min. In the cancer-patient serum experiment, the as-received serum samples were flowed into IBBCs without any pre-treatment (that is, no purification or dilution). Afterwards, a mixture of biotin-labeled detection antibodies (~50–100 nM) for the entire protein panel and the fluorescence Cy5-streptavidin conjugates (~100 nM) were flowed sequentially into IBBCs to complete the DEAL immunoassay. The unbound fluorescence probes were rinsed off by flowing the buffer solution for 10 min. At last, the PDMS chip was removed from the glass slide. The slide was immediately rinsed in $^1/_2\times$ PBS solution and deionized water and then dried with a nitrogen gun. Finally, the DEAL barcode slide was scanned by a microarray scanner.

Quantification and statistics. All the barcode array slides used in quantification were scanned using an Axon Genepix 4000B two-color laser microarray scanner at the same instrumental settings—100% and 33% for the laser power of 635 nm and 532 nm, respectively. Optical gains are 800 and 700 for 635 nm and 532 nm, respectively. The brightness and contrast were set at 87 and 88. The output JPEG images were carefully skewed and resized to fit the standard mask design of barcode array. Then, an image processing software, NIH imageJ, was used to produce intensity line profiles of barcodes in all assay channels. Finally, all the line profile data files were loaded into a home-developed program embedded as an Excel macro to generate a spreadsheet that lists the average intensities of all 13 bars in each of 20 barcodes. The means and standard divisions were computed using the Microcal origin. Nonsupervised clustering of patients was performed using the literature methods and algorithms[33]. To assess the significance of two patient (sub)groups, Student *t* analysis was performed on selected proteins and all *P*-values were calculated at a significance level of 0.05, if not otherwise specified.

Full methods and other supporting data are available in **Supplementary Methods** and **Supplementary Data** online.

Note: Supplementary information is available on the Nature Biotechnology website.

ACKNOWLEDGMENTS

The authors thank Larry Nagahara and Chris McLeland at the National Cancer Institute (NCI) for providing standard hCG serum samples and requesting the independent hCG measurement. We also thank Bruz Marzolf at the Institute for Systems Biology (Seattle) for printing DNA microarrays, and the UCLA nanolab for photomask fabrication. This work was funded by the National Cancer Institute grant no. 5U54 CA119347 (J.R.H., P.I.) and by the Institute for Collaborative Biotechnologies through grant DAAD19-03-D-0004 from the US Army Research Office.

AUTHOR CONTRIBUTIONS

R.F. developed and validated the DEAL barcode assay, measured cancer patient serum samples and analyzed all data. O.V. and B.K.H.Y. developed the blood separation chip. O.V., A.S. and L.Q. performed finger-prick blood test. R.F., O.V., A.S., H.A., G.A.K., C.-C.L. and J.G. participated in the synthesis and validation of reagents and the patterning of DNA barcode microarrays. L.H. and J.R.H. designed and directed the project.

COMPETING INTERESTS STATEMENT

The authors declare competing financial interests: details accompany the full-text HTML version of the paper at http://www.nature.com/naturebiotechnology/

Published online at http://www.nature.com/naturebiotechnology/
Reprints and permissions information is available online at http://npg.nature.com/reprintsandpermissions/

1. Anderson, N.L. & Anderson, N.G. The human plasma proteome: history, character, and diagnostic prospects. *Mol. Cell. Proteomics* **1**, 845–867 (2002).
2. Fujii, K. *et al.* Clinical-scale high-throughput human plasma proteome clinical analysis: Lung adenocarcinoma. *Proteomics* **5**, 1150–1159 (2005).
3. Lathrop, J.T., Anderson, N.L., Anderson, N.G. & Hammond, D.J. Therapeutic potential of the plasma proteome. *Curr. Opin. Mol. Ther.* **5**, 250–257 (2003).
4. Chen, J.H. *et al.* Plasma proteome of severe acute respiratory syndrome analyzed by two-dimensional gel electrophoresis and mass spectrometry. *Proc. Natl. Acad. Sci. USA* **101**, 17039–17044 (2004).
5. Hsieh, S.Y., Chen, R.K., Pan, Y.H. & Lee, H.L. Systematical evaluation of the effects of sample collection procedures on low-molecular-weight serum/plasma proteome profiling. *Proteomics* **6**, 3189–3198 (2006).
6. Sia, S.K. & Whitesides, G.M. Microfluidic devices fabricated in poly(dimethylsiloxane) for biological studies. *Electrophoresis* **24**, 3563–3576 (2003).
7. Quake, S.R. & Scherer, A. From micro- to nanofabrication with soft materials. *Science* **290**, 1536–1540 (2000).
8. Huang, B. *et al.* Counting low-copy number proteins in a single cell. *Science* **315**, 81–84 (2007).
9. Ottesen, E.A., Hong, J.W., Quake, S.R. & Leadbetter, J.R. Microfluidic digital PCR enables multigene analysis of individual environmental bacteria. *Science* **314**, 1464–1467 (2006).
10. Huang, L.R., Cox, E.C., Austin, R.H. & Sturm, J.C. Continuous particle separation through deterministic lateral displacement. *Science* **304**, 987–990 (2004).
11. Chou, C.F. *et al.* Sorting biomolecules with microdevices. *Electrophoresis* **21**, 81–90 (2000).
12. Toner, M. & Irimia, D. Blood-on-a-chip. *Annu. Rev. Biomed. Eng.* **7**, 77–103 (2005).
13. Nagrath, S. *et al.* Isolation of rare circulating tumour cells in cancer patients by microchip technology. *Nature* **450**, 1235–1239 (2007).
14. Yang, S., Undar, A. & Zahn, J.D. A microfluidic device for continuous, real time blood plasma separation. *Lab Chip* **6**, 871–880 (2006).
15. Svanes, K. & Zweifach, B.W. Variations in small blood vessel hematocrits produced in hypothermic rates by micro-occlusion. *Microvasc. Res.* **1**, 210–220 (1968).
16. Fung, Y.C. Stochastic flow in capilary blood vessels. *Microvasc. Res.* **5**, 34–38 (1973).
17. Bailey, R.C., Kwong, G.A., Radu, C.G., Witte, O.N. & Heath, J.R. DNA-encoded antibody libraries: a unified platform for multiplexed cell sorting and detection of genes and proteins. *J. Am. Chem. Soc.* **129**, 1959–1967 (2007).
18. Boozer, C., Ladd, J., Chen, S.F. & Jiang, S.T. DNA-directed protein immobilization for simultaneous detection of multiple analytes by surface plasmon resonance biosensor. *Anal. Chem.* **78**, 1515–1519 (2006).
19. Niemeyer, C.M. Functional devices from DNA and proteins. *Nano Today* **2**, 42–52 (2007).
20. Pirrung, M.C. How to make a DNA chip. *Angewandte Chemie-International Edition* **41**, 1276–1289 (2002).
21. Coussens, L.M. & Werb, Z. Inflammation and cancer. *Nature* **420**, 860–867 (2002).
22. Lin, W.W. & Karin, M. A cytokine-mediated link between innate immunity, inflammation, and cancer. *J. Clin. Invest.* **117**, 1175–1183 (2007).
23. De Marzo, A.M. *et al.* Inflammation in prostate carcinogenesis. *Nat. Rev. Cancer* **7**, 256–269 (2007).
24. Ashton, H. & Telford, R. Smoking and carboxhemoglobin. *Lancet* **2**, 857–858 (1973).
25. Chopra, V., Dinh, T.V. & Hannigan, E.V. Serum levels of interleukins, growth factors and angiogenin in patients with endometrial cancer. *J. Cancer Res. Clin. Oncol.* **123**, 167–172 (1997).
26. Oncul, O., Top, C. & Cavuplu, P. Correlation of serum leptin levels with insulin sensitivity in patients with chronic hepatitis-C infection. *Diabetes Care* **25**, 937 (2002).
27. Pinsky, M.R. *et al.* Serum cytokine levels in human septic shock: relation to multiple-system organ failure and mortality. *Chest* **103**, 565–575 (1993).
28. Schweitzer, B. *et al.* Multiplexed protein profiling on microarrays by rolling-circle amplification. *Nat. Biotechnol.* **20**, 359–365 (2002).
29. Lambeck, A.J.A. *et al.* Serum cytokine profiling as a diagnostic and prognostic tool in ovarian cancer: A potential role for interleukin 7. *Clin. Cancer Res.* **13**, 2385–2391 (2007).
30. Gorelik, E. *et al.* Multiplexed immunobead-based cytokine profiling for early detection of ovarian cancer. *Cancer Epidemiol. Biomarkers Prev.* **14**, 981–987 (2005).
31. Heath, J.R. & Davis, M.E. Nanotechnology and cancer. *Annu. Rev. Med.* **59**, 251–265 (2008).
32. Zimmermann, M., Delamarche, E., Wolf, M. & Hunziker, P. Modeling and optimization of high-sensitivity, low-volume microfluidic-based surface immunoassays. *Biomed. Microdevices* **7**, 99–110 (2005).
33. Eisen, M.B., Spellman, P.T., Brown, P.O. & Botstein, D. Cluster analysis and display of genome-wide expression patterns. *Proc. Nat. Acad. Sci. USA* **95**, 14863–14868 (1998).